The Reactions of *arachno*-Decaboranyl Complexes $L_2B_{10}H_{12}$ (L = Two-electron Donor Ligand) with some Platinum(II) Compounds; Nuclear Magnetic Resonance Studies and the Crystal and Molecular Structure of [8-Cl-7,7-$(PMe_2Ph)_2$-*nido*-7-$PtB_{10}H_{11}$] *

Janet E. Crook, Norman N. Greenwood, John D. Kennedy, and Walter S. McDonald
Department of Inorganic and Structural Chemistry, University of Leeds, Leeds LS2 9JT

The reactions of *arachno*-6,9-$(SMe_2)_2B_{10}H_{12}$ and of *arachno*-6,9-$(MeCN)_2B_{10}H_{12}$ with the complex *cis*-[$PtCl_2(PMe_2Ph)_2$] give moderate yields of the *nido*-platinaundecaborane [8-Cl-7,7-$(PMe_2Ph)_2$-7-$PtB_{10}H_{11}$] which has been characterised by single-crystal *X*-ray diffraction analysis. Analogous reactions with the dimeric species [{$PtCl_2(PR_3)$}$_2$] (R_3 = $Me_{3-n}Ph_n$, *n* = 0, 1, or 2), by contrast, give the *nido*-platinaundecaboranes [7-Cl-7-(PR_3)-8-(SMe_2)-7-$PtB_{10}H_{11}$] which have been characterized by single- and multiple-resonance n.m.r. spectroscopy. Additional products of the reactions include the *arachno* nine-vertex species 4-$(MeCN)B_9H_{13}$ and 4-$(SMe_2)B_9H_{13}$.

A rich metallaborane chemistry results from the reaction of *nido*-decaborane with a variety of transition metal species.[1] A typical example pertinent to this work is the reaction of $B_{10}H_{14}$ with *cis*-[$PtCl_2(PMe_2Ph)_2$] in the presence of base (Y) to give a high yield of the *nido*-metallaundecaborane [$(PMe_2Ph)_2PtB_{10}H_{12}$] [equation (i)]; this and related reactions have

$$[PtCl_2(PMe_2Ph)_2] + B_{10}H_{14} + 2Y \longrightarrow [(PMe_2Ph)_2PtB_{10}H_{12}] + 2HY^+Cl^- \qquad (i)$$

generated much interesting chemistry.[2-7] By contrast, although *nido*-$B_{10}H_{14}$ can be readily converted in high yield [8] to the *arachno* species $L_2B_{10}H_{12}$ (where L is a two-electron donor ligand), the reactions of these latter compounds with transition metal complexes have been relatively little investigated. As far as we are aware, investigations with *arachno*-decaboranes in this area have been limited to that of the platinum(0) compound [$Pt(PPh_3)_3$] with $(SEt_2)_2B_{10}H_{12}$ [9] and that of $PtCl_2$, or [$Pd(cod)I_2$] (cod = cyclo-octa-1,5-diene), with $Cs_2B_{10}H_{14}$,[10] which give small yields of the *nido*-metallaundecaboranes [$(PPh_3)_2PtB_{10}H_{12}$] and [$Pt(B_{10}H_{12})_2$]$^{2-}$ respectively. Here, therefore, we now present more detailed work on the interactions of selected *arachno*-bis(ligand)decaborane species, $L_2B_{10}H_{12}$ (L = SMe_2, MeCN, or PMe_2Ph), with platinum(II) chloride complexes of tertiary phosphine ligands such as PMe_2Ph.

In this paper we use the conventional IUPAC recommended numbering systems [structures (1)—(3)] for the nine-, ten-, and eleven-vertex open clusters discussed: [11] it may be noted that successive addition of atoms as additional vertices generally changes the numbering of a particular atom within the cluster.

Results and Discussion

In dichloromethane solution, the ten-vertex species *arachno*-bis(dimethyl sulphide)decaborane(14), 6,9-$(SMe_2)_2B_{10}H_{12}$, reacts completely with an equivalent amount of *cis*-[$PtCl_2(PMe_2Ph)_2$] in *ca.* 36 h at room temperature or *ca.* 3 h at reflux temperatures. A number of products are formed, of which we have been able to identify two as metallaborane species. Of these, the minor component, a yellow crystalline compound obtained in 6% yield, is readily identified as the eleven-vertex species [7,7-$(PMe_2Ph)_2$-*nido*-7-$PtB_{10}H_{12}$] by its detailed ^{31}P, ^{11}B, and ^1H single- and multiple-resonance n.m.r. behaviour with which we are very familiar.[2-4] The major component, also an air-stable yellow crystalline solid (18% yield), m.p. *ca.* 170 °C (decomp.), appeared from elemental analytical data to be a chlorinated bis(dimethylphenylphosphine)platiniodecaborane species, and its n.m.r. properties suggested that it was probably an eleven-vertex-*nido*-7-platinaundecaborane compound. The borane-cage ^{11}B and ^1H n.m.r. data are summarized in Table 1. Ten separate boron resonance signals were observed, and selective ^1H-{^{11}B} experiments showed that nine of these had terminal H atoms associated with them and that in addition there were two B–H–B bridging H atoms. At low temperatures two different phosphorus environments were apparent. Preliminary application of the chemical shift additivity principles being developed concurrently with this work in these laboratories [7] suggested that the compound was in fact the eleven-vertex 8-chloro-derivative, *viz.* [8-Cl-7,7-$(PMe_2Ph)_2$-*nido*-7-$PtB_{10}H_{11}$]. That

Table 1. Proton and boron-11 n.m.r. data for [$(PMe_2Ph)_2PtB_{10}H_{11}Cl$] at +21 °C

Assignment of position	$\delta(^{11}B)$ [a]/p.p.m.	$\delta(^1H)$ [b]/p.p.m.	$^nJ(^{195}Pt-^1H)$/Hz
(6)	−30.7	+1.03	56 ± 4
(4)	−21.2	+1.83	*c*
(9)	−7.4	+2.45	—
(10)	−0.8	+2.49	—
(1)	+1.2	+2.68	—
(11)	+4.4 [d]	+3.17	*d*
(3)	+5.01 [d]	+2.79	*d*
(5)	+12.9	+3.37	*ca.* 70 (?)
(8)	+19.5 [e]	—	—
(2)	+22.1 [f]	+4.10	36 ± 4
(8)/(9) (bridge)	—	−0.05	46 ± 4
(10)/(11) (bridge)	—	−2.64	65 ± 5

[a] In $CDCl_3$ solution; $\delta(^{11}B)$ ±0.5 p.p.m. to high frequency (low field) of $BF_3{\cdot}OEt_2$ in $CDCl_3$. [b] In CD_2Cl_2 solution; $\delta(^1H)$ ±0.08 p.p.m. to high frequency (low field) of $SiMe_4$. [c] Any $^3J(^{195}Pt-^1H)$ not observed due to lines in ^1H spectrum of PMe_2Ph also being perturbed in ^1H-{^{11}B} experiments (see also ref. 19) and thus obscuring the fine structure on the overlapping $^1H(4)$ resonance. [d] Any $^1J(^{195}Pt-^{11}B)$ and $^2J(^{195}Pt-^1H)$ not observed due to overlapping resonances. [e] $^1J(^{195}Pt-^{11}B)$ = 310 ± 60 Hz. [f] $^1J(^{195}Pt-^{11}B)$ = 280 ± 30 Hz.

---

* 8-Chloro-7,7-bis(dimethylphenylphosphine)-*nido*-7-platinaundecaborane.

Supplementary data available (No. SUP 56036, 2 pp.): thermal parameters. See Instructions for Authors, *J. Chem. Soc., Dalton Trans.*, 1984, Issue 1, pp. xvii—xix. Structure factors are available from the editorial office.

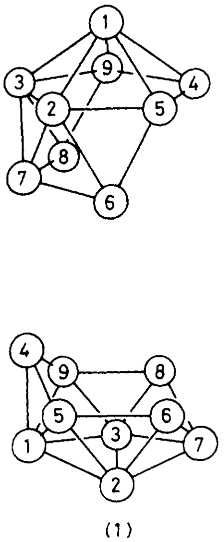

(1)

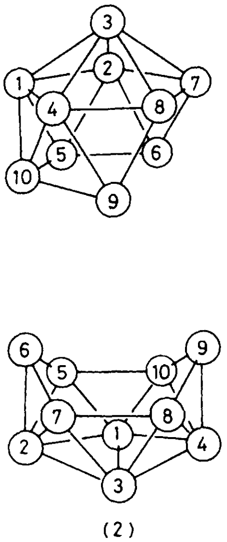

(2)

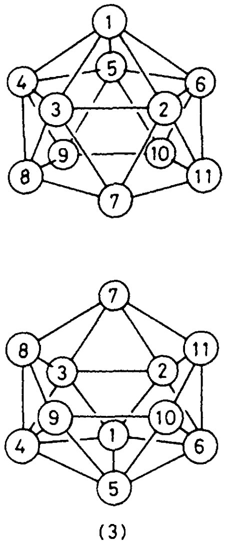

(3)

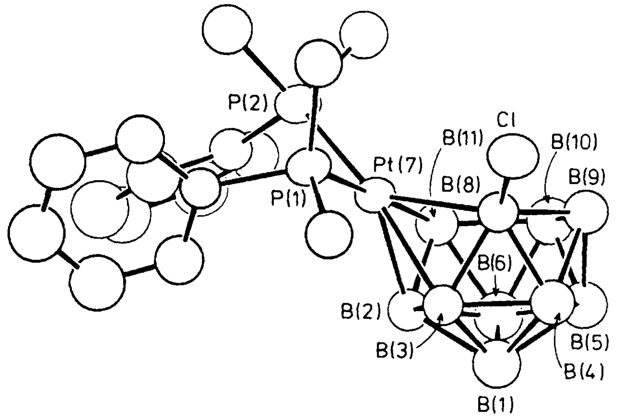

Figure 1. ORTEP drawing of the molecular structure of [8-Cl-7,7-$(PMe_2Ph)_2$-7-$PtB_{10}H_{11}$]. Hydrogen atoms were not located, but the presence of terminal hydrogen atoms on all boron atoms except B(8), and the presence of bridging hydrogen atoms at B(8)/B(9) and and B(10)/B(11), are reasonably inferred from n.m.r. spectroscopy (Table 1 and text)

this was indeed the case has been confirmed by single-crystal *X*-ray diffraction analysis.

The molecular structure is shown in Figure 1, selected interatomic distances in Table 2, and angles between interatomic vectors in Table 3. Atomic co-ordinates are presented in the Experimental section. Hydrogen atoms were not located but the presence of nine terminal B–H hydrogen atoms and two bridging B–H–B hydrogen atoms readily followed from n.m.r. spectroscopy as briefly mentioned above and summarized in Table 1.

The eleven-vertex platinaborane cage structure closely resembles that of the unsubstituted cage in the parent compound $[(PMe_2Ph)_2PtB_{10}H_{12}]$ and that in the 4-(2′-$B_{10}H_{13}$) substituted cage of $[(PMe_2Ph)_2PtB_{20}H_{24}]$.[4] There is no significant alteration in the interatomic distances associated with the substituted boron atom B(8) when compared with those in the unsubstituted compound $[(PMe_2Ph)_2PtB_{10}H_{12}]$. Although a few others, *e.g.* B(2)–B(3), B(9)–B(10), and B(10)–B(11) appear to be slightly longer, this may well arise because H atoms were located and refined in the unchlorinated compound but not in the species reported here.

Table 2. Interatomic distances (pm) for $[(PMe_2Ph)_2PtB_{10}H_{11}Cl]$ with estimated standard deviations in parentheses *

(*i*) From the platinum atom			
Pt(7)–P(1)	232.5(3)	Pt(7)–P(2)	235.4(3)
Pt(7)–B(3)	224.1(13)	Pt(7)–B(2)	220.6(12)
Pt(7)–B(8)	227.1(13)	Pt(7)–B(11)	234.2(13)
(*ii*) Boron–boron			
B(1)–B(2)	178.2(19)	B(1)–B(3)	175.9(18)
B(1)–B(5)	179.0(20)		
B(1)–B(6)	177.8(21)	B(1)–B(4)	180.1(20)
B(2)–B(3)	185.1(18)	B(9)–B(10)	195.1(21)
B(2)–B(6)	179.4(19)	B(3)–B(4)	178.8(18)
B(2)–B(11)	181.0(18)	B(3)–B(8)	178.7(18)
B(5)–B(6)	176.0(21)	B(4)–B(5)	178.8(19)
B(5)–B(10)	177.0(21)	B(5)–B(9)	175.6(19)
B(6)–B(10)	177.3(21)	B(4)–B(9)	177.8(19)
B(6)–B(11)	179.9(18)	B(4)–B(8)	173.1(17)
B(10)–B(11)	185.2(20)	B(8)–B(9)	179.9(18)
(*iii*) Phosphorus–carbon			
P(1)–C(11)	181.2(6)	P(2)–C(21)	182.8(7)
P(1)–Me(11)	183.7(12)	P(2)–Me(21)	187.0(12)
P(1)–Me(12)	184.2(12)	P(2)–Me(22)	181.5(12)
(*iv*) Other			
B(8)–Cl	184.1(13)		

* The phenyl rings were constrained to C–C 139.5 pm and C–C–C 120°.

It is, however, difficult to distinguish asymmetric effects in the molecule due to the chlorine substituent from effects due to the 'twist' distortion from ideal P_2PtB_{10} C_s symmetry apparent from the disposition of the two phosphine ligands in Figure 2. The distortion presumably arises from crystal packing forces, and, in this instance, perhaps also from a steric contribution from the Cl substituent on the B(8) atom, and is illustrated in Figure 2, which views the P(1)P(2)Pt(7)-B(8)B(3)B(2)B(11) system in the Pt(7)P(1)P(2) plane. It is of interest that the angle of distortion from ideal C_2 symmetry ($\theta = 24°$ as defined in refs. 2 and 4) is somewhat greater than that observed[4] for $[(PMe_2Ph)_2PtB_{20}H_{24}]$ (8°) and $[(PMe_2Ph)_2PtB_{10}H_{12}]$ (20°). However, it should be pointed out that these

Table 3. Selected angles (°) between the interatomic vectors with estimated standard deviations in parentheses for [$(PMe_2Ph)_2PtB_{10}H_{11}Cl$]

(*i*) At the platinum atom

P(1)–Pt(7)–P(2)	96.1(1)		
P(1)–Pt(7)–B(2)	132.9(3)	P(2)–Pt(7)–B(2)	114.8(4)
P(1)–Pt(7)–B(3)	95.8(3)	P(2)–Pt(7)–B(3)	163.9(3)
P(1)–Pt(7)–B(8)	93.0(3)	P(2)–Pt(7)–B(8)	143.1(3)
P(1)–Pt(7)–B(11)	177.9(3)	P(2)–Pt(7)–B(11)	82.7(3)
B(2)–Pt(7)–B(3)	49.2(5)	B(8)–Pt(7)–B(11)	89.0(5)
B(2)–Pt(7)–B(8)	83.1(5)	B(3)–Pt(7)–B(11)	85.1(4)
B(2)–Pt(7)–B(11)	46.8(5)	B(3)–Pt(7)–B(8)	46.7(5)

(*ii*) Platinum–boron–boron

Pt(7)–B(2)–B(1)	118.0(8)	Pt(7)–B(3)–B(1)	117.3(8)
Pt(7)–B(2)–B(3)	66.4(6)	Pt(7)–B(3)–B(2)	64.4(5)
Pt(7)–B(2)–B(6)	120.5(8)	Pt(7)–B(3)–B(4)	118.1(8)
Pt(7)–B(2)–B(11)	70.6(6)	Pt(7)–B(3)–B(8)	67.5(6)
Pt(7)–B(11)–B(2)	62.7(6)	Pt(7)–B(8)–B(3)	65.8(6)
Pt(7)–B(11)–B(6)	113.6(8)	Pt(7)–B(8)–B(4)	119.2(8)
Pt(7)–B(11)–B(10)	111.8(8)	Pt(7)–B(8)–B(9)	115.5(8)

(*ii*) Boron–boron–boron

Range: 56.0—67.2 (mean 60.0)
Range: 104.5—115.7 (mean 109.2)

(*iv*) Other

Pt(7)–B(8)–Cl	115.7(6)	B(4)–B(8)–Cl	119.4(9)
B(3)–B(8)–Cl	128.3(8)	B(9)–B(8)–Cl	114.5(8)
Pt(7)–P(1)–C(11)	108.7(3)	Pt(7)–P(2)–C(21)	116.0(3)
Pt(7)–P(1)–Me(11)	117.5(4)	Pt(7)–P(2)–Me(21)	119.5(4)
Pt(7)–P(1)–Me(12)	118.3(4)	Pt(7)–P(2)–Me(22)	111.3(4)

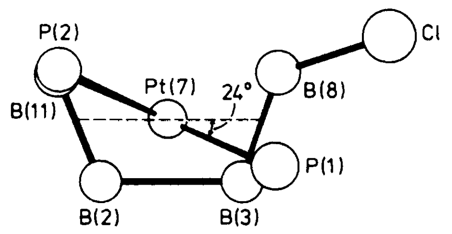

Figure 2. View in the Pt(7)P(1)P(2) plane of the platinum and circumjacent atoms of [$8\text{-}Cl\text{-}7,7\text{-}(PMe_2Ph)_2\text{-}7\text{-}PtB_{10}H_{11}$]. The angle θ (as defined in refs. 2 and 4) is about 24°, as indicated

differences will arise principally from different packing effects within the three crystals, and are not necessarily dependent on the energy barrier for complete rotation (*i.e.* θ passing through 90°) discussed in the following paragraph.

Table 4. Phosphorus-31 [a] and proton n.m.r. data for the P-methyl groups of [$8\text{-}Cl\text{-}7,7\text{-}(PMe_2Ph)_2\text{-}7\text{-}PtB_{10}H_{11}$] [b]

Temp. (solvent)	$\delta(^1H)$/p.p.m.	$^3J(^{195}Pt-^1H)$ (approx.)/Hz	$(^2J + {}^4J)(^{31}P-^1H)$ (approx.)/Hz
+72 °C (C_6D_6)	+1.45 (A)	24.2 (A)	10.1 (A)
	+1.02 (B)	22.0 (B)	9.6 (B)
+21 °C (CD_2Cl_2)	+1.96 (A)	24.9 (A)	9.8 (A)
	+1.63 (B)	22.9 (B)	*ca.* 10 (B)
−45 °C (CD_2Cl_2)	+1.84 (A1)	*ca.* 28 (A1)	*c*
	+2.10 (A2)	*ca.* 23 (A2)	*c*
	+1.33 (B1)	*ca.* 28 (B1)	*c*
	+1.75 (B2)	*ca.* 20 (B2)	*c*

[a] Additional phosphorus-31 data: $\delta(^{31}P) = +2.3$ p.p.m. (both resonances accidently equivalent), $^2J(^{31}P-^{31}P) = 32$; $^1J(^{195}Pt-^{31}P) =$ 2 446 and 2 657 Hz ($CDCl_3$ solution at −51 °C). [b] A, B, A1, B1, A2, and B2 designate chemically inequivalent methyl groups. [c] Not measured.

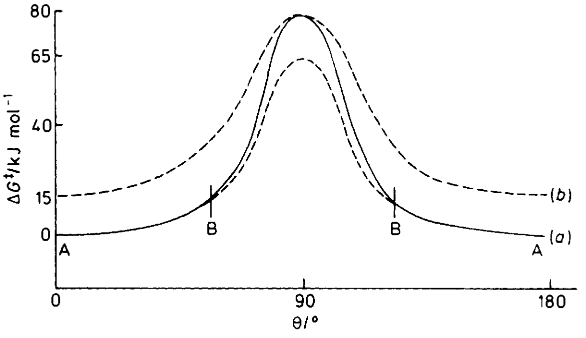

Figure 3. Schematic representation of energy barriers to the twist contrarotation of the $(PMe_2Ph)_2$ and $B_{10}H_{11}X$ groupings about the platinum atom in [$7,7\text{-}(PMe_2Ph)_2\text{-}7\text{-}PtB_{10}H_{12}$] (———) and [$8\text{-}Cl\text{-}7,7\text{-}(PMe_2Ph)_2\text{-}7\text{-}PtB_{10}H_{11}$] (– – –): (*a*) electronic effect of Cl, (*b*) effect of non-bonding interaction of Cl with PMe_2Ph ligand

As in other eleven-vertex bis(phosphine)platinaundecaboranes reported previously from these laboratories,[2,4] in the liquid phase the metal-to-borane bonding in [$8\text{-}Cl\text{-}7,7\text{-}(PMe_2Ph)_2\text{-}7\text{-}PtB_{10}H_{11}$] is rotationally fluxional, the rotation being represented by θ of Figure 2 increasing through 90 and 180° to interchange the chemical environments of the two phosphine ligands.[4] The ^1H and ^{31}P n.m.r. parameters for the dimethylphenylphosphine ligands are summarized in Table 4. At lower temperatures, four chemically inequivalent P-methyl-proton resonance patterns are observed, but these coalesce in pairs to give two resonance patterns at higher temperatures, the peak separations and coalescence temperatures of 268 and 270 K yielding a value for $\Delta G^{\ddagger}$ of 56 ± 2 kJ mol^{-1} for the rotational process at these temperatures. This is somewhat lower than the values observed for the previously investigated[4] non-halogenated platinaundecaboranes, but it is not clear whether this arises predominantly from an effective decrease in energy of the transition state at θ = *ca.* 90° resulting from the electronic effect of the electronegative chlorine substituent [dashed part of curve (*a*) in Figure 3] or from an effective increase in energy of the ground state at low θ [dashed curve (*b*) in Figure 3] resulting essentially from non-bonding interaction between the bulkier halogen atom and the dimethylphenylphosphine group. These rotational effects are presented for a more comprehensive series of halogen-substituted *nido*-7-platinaundecaboranes elsewhere.[7] The various 'twist' angles in the solid-state molecular structures discussed in the previous paragraph will represent successive initial stages of the rotation, and will probably lie on the lower parts AB ($\Delta G <$ *ca.* 10 kJ mol^{-1}) of curves such as that shown schematically in Figure 3.

Additional products are present in the reaction that yields [$8\text{-}Cl\text{-}7,7\text{-}(PMe_2Ph)_2\text{-}7\text{-}PtB_{10}H_{11}$], of which the unsubstituted eleven-vertex species [$7,7\text{-}(PMe_2Ph)_2\text{-}7\text{-}PtB_{10}H_{12}$] has been mentioned above. T.l.c. analysis showed that the distribution of the other (non-platinum-containing) products is comparable to that resulting from the decomposition of $(SMe_2)_2B_{10}H_{12}$ when this is maintained under the same reaction conditions, but in the *absence* of [$PtCl_2(PMe_2Ph)_2$]. Predominant among these other products is the *arachno* nine-vertex species 4-$(SMe_2)B_9H_{13}$, obtained in *ca.* 14% yield from the platinum reaction, and identified by n.m.r. spectroscopy as described below. Other products are present in much smaller quantities, and have not been identified unequivocally; some of these are presumably species such as $(SMe_2)B_{10}H_{12}$ and related compounds.[12-17]

A number of variations on this experiment have been investigated. (*i*) The use of Et_2O–CH_2Cl_2 (1 : 1 v/v) as solvent gives results similar to those above, though with substantially reduced yields of $[8\text{-}Cl\text{-}7,7\text{-}(PMe_2Ph)_2\text{-}7\text{-}PtB_{10}H_{11}]$ and the concurrent formation of the known [6,18,19] nine-vertex species $[(PMe_2Ph)_2PtB_8H_{12}]$ (15%) and fourteen-vertex species $[(PMe_2Ph)_2Pt_2B_{12}H_{18}]$ (<1%), both readily identified by n.m.r. spectroscopy. These last two compounds are known [6,19-21] to be products of reactions of $[PtCl_2(PMe_2Ph)_2]$ with *arachno*-nonaborane species under basic conditions. Small amounts of *nido*-$B_{10}H_{14}$ are also formed. (*ii*) The use of stronger donor solvents such as tetrahydrofuran or methyl cyanide results in no significant reaction even after several days at room temperature. (*iii*) Similarly, the use of the very stable bis(ligand) *arachno* compound $(PMe_2Ph)_2B_{10}H_{12}$ instead of $(SMe_2)_2B_{10}H_{12}$ results in no significant reaction, even under quite forcing conditions (*e.g.* 110 °C in toluene), presumably because of the much greater donor strength of the phosphine ligand which in these compounds precludes a precursive dissociation of the boron–phosphorus bond. (*iv*) The use of the weaker ligand adduct $(MeCN)_2B_{10}H_{12}$ in CH_2Cl_2 as solvent gives comparable results to the reaction of the SMe_2 adduct: $[8\text{-}Cl\text{-}7,7\text{-}(PMe_2Ph)_2\text{-}7\text{-}PtB_{10}H_{11}]$ is produced in 15% yield, and $4\text{-}(MeCN)B_9H_{13}$, again identified by n.m.r. spectroscopy (see below), in ~2% yield.

Other variations and control reactions have also been examined. (*v*) The reaction between *cis*-$[PtCl_2(SMe_2)_2]$ and $(SMe_2)_2B_{10}H_{12}$ in CH_2Cl_2 solution gave a black suspension/solution which contained largely intractable products. (*vi*) A solution of $4\text{-}(SMe_2)B_9H_{13}$ and $[PtCl_2(PMe_2Ph)_2]$ in CH_2Cl_2 showed no significant reaction after two weeks at 21 °C, although it is known that in the presence of base the nine-vertex compound $[(PMe_2Ph)_2PtB_8H_{12}]$ and other degradation products are formed.[19-21] (*vii*) Heating under reflux of a solution of $[PtCl_2(PMe_2Ph)_2]$ and *nido*-$B_{10}H_{14}$ in CH_2Cl_2 resulted after 5 d in a reasonable yield (*ca.* 60%, 0.05 mmol) of the unchlorinated platinaundecaborane $[(PMe_2Ph)_2PtB_{10}H_{12}]$.

This last result is of more general interest as the production of eleven-vertex metallaboranes from metal halides and *nido*-$B_{10}H_{14}$ has been generally presumed to require basic conditions [*e.g.* equation (i) above] and to proceed *via* the $[B_{10}H_{13}]^-$ anion; that the reaction proceeds under not particularly basic conditions now introduces the possibility of an initial oxidative addition followed by elimination of HCl to give the product: equations (ii), (iiia), and (iiib).

$$[PtCl_2(PMe_2Ph)_2] + B_{10}H_{14} \longrightarrow \{HPtCl_2(B_{10}H_{13})(PMe_2Ph)_2\} \qquad (ii)$$

$$\{HPtCl_2(B_{10}H_{13})(PMe_2Ph)_2\} \xrightarrow{-HCl} \{PtCl(B_{10}H_{13})(PMe_2Ph)_2\} \qquad (iiia)$$

$$\{PtCl(B_{10}H_{13})(PMe_2Ph)_2\} \xrightarrow{-HCl} [(PMe_2Ph)_2PtB_{10}H_{12}] \qquad (iiib)$$

Most of the other results mentioned above are of more relevance in interpreting the new chemistry reported in this paper. That no reaction occurs either with strong ligand adducts such as $(PMe_2Ph)_2B_{10}H_{12}$, or in the presence of stronger donor solvents, suggests that there is a precursive equilibrium, equation (iv), as is believed to be the case for

$$L_2B_{10}H_{12} \rightleftharpoons LB_{10}H_{12} + L \qquad (iv)$$

many reactions undergone by these species.[6,13-17,22-25] This yields the 'reactive' form [15] of $9\text{-}(SMe_2)B_{10}H_{12}$ which is thought to have a *nido* ten-vertex cage electron cluster count with a vacant and presumably reactive co-ordination site at the 6-position which will be susceptible to nucleophilic attack. This intermediate might be stabilized by formation of a 6,9-μ-SMe_2-bridged species.[26] With hydrogen chloride, this then reacts to give $6\text{-}ClB_{10}H_{13}$.[22-25] The equivalent stage in the reaction with $[PtCl_2(PMe_2Ph)_2]$ may also involve an attack by $Cl^{\delta-}$ at this position followed by displacement of SMe_2 and elimination of HCl [perhaps as in equations (iiia) or (iiib) above] to give the product; *i.e.* there may be general parallels between the reaction of the H–Cl and of the Pt–Cl bonds with the decaboranyl cage in this case. The overall stoicheiometry is represented in equation (v). However, an initial attack by the platinum

$$[PtCl_2(PMe_2Ph)_2] + (SMe_2)_2B_{10}H_{12} \longrightarrow [(PMe_2Ph)_2PtB_{10}H_{11}Cl] + HCl + 2\,SMe_2 \qquad (v)$$

centre cannot be ruled out on this limited evidence, especially in the light of the nature of the products from the reaction of $(SMe_2)_2B_{10}H_{12}$ with the dimeric monophosphine platinum dihalide species $[\{PtCl_2(PMe_2Ph)\}_2]$ [variation (*viii*)]. In dichloromethane solution, these two last compounds react completely over 36 h at room temperature, and over 3 h at reflux temperature. As with the reaction of $[PtCl_2(PMe_2Ph)_2]$ discussed above, the nine-vertex species *arachno*-$[4\text{-}(SMe_2)B_9H_{13}]$ and other decomposition products of $(SMe_2)_2B_{10}H_{12}$ are formed, but the predominant product, formed in up to 70% yield, is a new metallaborane compound, isolable in 14% yield as a yellow powdery solid. Although reasonably stable under N_2 in the solid state, this new product is not as robust as the 8-chloro-7-platinaundecaborane discussed above (Figure 1), and it decomposes readily in solution, especially in the presence of air, to give $4\text{-}(SMe_2)B_9H_{13}$ as the main characterizable decomposition product. The complexes *trans*-$[\{PtCl_2(PMe_3)\}_2]$ and *trans*-$[\{PtCl_2(PMePh_2)\}_2]$ react similarly to give analogous compounds (although the product from the $PMePh_2$ reaction appears to be much less stable than the others), and use of $(MeCN)_2B_{10}H_{12}$ instead of $(SMe_2)_2B_{10}H_{12}$ also gives the analogous product which yields $4\text{-}(MeCN)B_9H_{13}$ when allowed to decompose.

Table 5. Proton n.m.r. data for the P-methyl and S-methyl groups of $[(PMe_2Ph)ClPtB_{10}H_{11}(SMe_2)]$ in $CDCl_3$ solution at +21 °C

$\delta(^1H)$/p.p.m.	$^2J(^{31}P-^1H)$/Hz	$^3J(^{195}Pt-^1H)$/Hz
2.01 (PMe)	10.5 ± 0.5	26.4 ± 1.0
1.91 (PMe)	9.3 ± 1.0	26.2 ± 1.0
2.74 (SMe) *	—	—
2.69 (SMe) *	—	—

* Height increase (*ca.* 24%) upon ^{11}B irradiation, implying a small coupling $^3J(^{11}B-S-C-^1H)$ of ≤ *ca.* 1 Hz.

These results indicate an interesting product in which the initial ligand (SMe_2 or MeCN) is still attached to the borane cage, but none of the compounds have proved suitable for single-crystal *X*-ray diffraction analysis for a variety of reasons. However, the constitution and structure are reasonably inferred from analytical and n.m.r. data. For example, for the product of the $(SMe_2)_2B_{10}H_{12}/[\{PtCl_2(PMe_2Ph)\}_2]$ reaction, analytical data were not inconsistent with molecular formulations $PtCl(B_{10}H_{11})(PMe_2Ph)(SMe_2)$, and integrated proton n.m.r. spectroscopy (Table 5) confirmed the presence and the 1 : 1 molecular ratio of the SMe_2 and PMe_2Ph ligands. Ten different ^{11}B n.m.r. signals were observed (Table 6), implying a structure with no symmetry, and selective $^1H\text{-}\{^{11}B\}$

Table 6. Boron, phosphorus, and selected proton n.m.r. data for $[(PMe_2Ph)ClPtB_{10}H_{11}(SMe_2)]$, in $CDCl_3$ solution at +21 °C [a]

Tentative assignment of position	$\delta(^{11}B)$/p.p.m.	$\delta(^{1}H)$/p.p.m.
(6)	−32.0	+1.26
(4)	−27.5	+0.99 [b]
(9)	−9.1	+2.55
(1)	−5.7	+2.52
(10)	−4.4	+2.60
(8)	+4.6	—
(3)	+7.0	+3.11
(11)	+7.2 [c]	+2.88
(5)	+14.9	+3.06
(2)	+16.0	+3.99
(8)/(9) (bridge)	—	−1.34 [d]
(10)/(11) (bridge)	—	−0.70 [e]

[a] $\delta(^{31}P)$ = +10.4 p.p.m., $^{1}J(^{195}Pt-^{31}P)$ = 2 440 Hz ($CDCl_3$ at −45 °C); $^{3}J(^{195}Pt-P-C-^{1}H)$(mean) = 26.3 Hz. Parameters for PMe_3 analogue are very similar: $\delta(^{11}B)$ within ±1 p.p.m. (+21 °C); $\delta(^{31}P)$ = +7.7 p.p.m.; $^{1}J(^{195}Pt-^{31}P)$ = 2 435 Hz ($CDCl_3$ at −55 °C). [b] $^{3}J(^{195}Pt-^{1}H)$ = *ca.* 65 Hz. [c] Approximate value only. [d] $^{2}J(^{195}Pt-^{1}H)$ = *ca.* 60 Hz. [e] $^{2}J(^{195}Pt-^{1}H)$ = *ca.* 40 Hz.

experiments [3,19,27] showed that nine of these had *exo*-terminal H atoms bound to them [*i.e.* one B atom, that at $\delta(^{11}B)$ = +4.6 p.p.m., had another substituent] and that there were in addition two open-face bridging B–H–B atoms present. The overall pattern of shielding and coupling-constant behaviour summarized in Table 6 is markedly similar to that found [3,4,7,9] for other eleven-vertex *nido*-7-platinaundecaboranes, reasonably implying that this compound also belongs to this structural class, and permitting the partial tentative assignments as indicated in Table 6. The couplings $^{1}J(^{195}Pt-^{31}P)$ (Table 5) are of the size expected [3,4,6,19,25,28] for straightforward $R_3P\rightarrow Pt$ ligation in platinaboranes, and the presence of couplings $^{2}J(^{195}Pt-P-C-^{1}H)$ in the P-methyl groups confirms that this is the case. No corresponding satellites expected [29] to arise from any couplings $^{3}J(^{195}Pt-S-C-^{1}H)$ were observed for the S-methyl proton resonances, however, indicating that the SMe_2 group is bonded not to the Pt atom but directly to the boron cage [presumably to the B atom with the n.m.r. signal at $\delta(^{11}B)$ = +4.6 p.p.m.]. This tends to be confirmed in that these S-methyl proton resonances are sharpened (from $w_{\frac{1}{2}}$ = *ca.* 3 to *ca.* 2.5 Hz, or *ca.* 24% increase in signal height) in ^{1}H-{^{11}B} experiments, implying the presence of a significant coupling, $^{3}J(^{11}B-S-C-^{1}H)$, and it is also consistent with a retention of the S–B linkage in the observed decomposition product $(SMe_2)B_9H_{13}$. The signal at $\delta(^{11}B)$ = 4.6 p.p.m. due to the SMe_2-substituted boron atom also exhibits satellite fine structure arising from a coupling with ^{195}Pt of *ca.* 260 Hz. A splitting of this magnitude implies [3,4,6,7,19,30] an *endo* one-bond coupling constant $^{1}J(^{195}Pt-^{11}B)$ which therefore assigns this resonance to the B(3) or B(8) position in the 7-platinaundecaborane cluster. That it is in the B(8) position is confirmed by the selective ^{11}B-{^{1}H(bridge)} experiments illustrated by Figure 4. Selective collapse of the coupling $^{1}J[^{11}B(8)-^{1}H(8,9\text{-bridge})]$ of *ca.* 20—30 Hz results in selective sharpening of the B(8) resonance; any coupling $^{2}J[^{11}B(3)-B(8)-^{1}H(8,9\text{-bridge})]$ would be much smaller and no significant effect is observed in ^{11}B-{^{1}H(bridge)} experiments such as these.

These considerations indicate an eleven-vertex *nido*-7-platinaundecaborane cluster with an SMe_2 substituent on the 8-position and PR_3 ligand on the platinum atom in the 7-position. This would leave a vacant co-ordination site on the platinum atom which is reasonably occupied by the Cl atom, apparent from the analytical data. The overall structure is

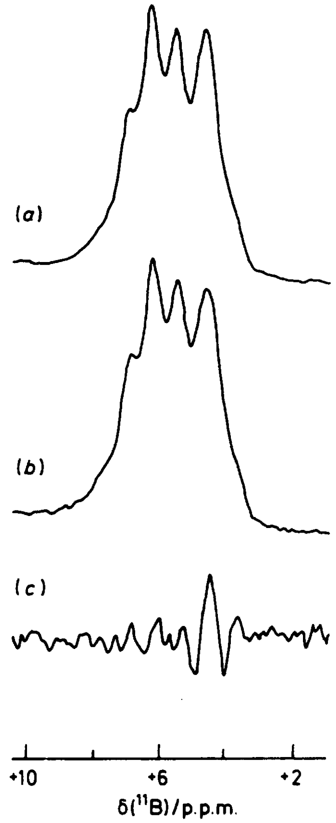

Figure 4. Boron-11 spectra (128 MHz) of the B(1)B(8)B(10) region for the trimethylphosphine compound $[8\text{-}(SMe_2)\text{-}7\text{-}(PMe_3)\text{-}7\text{-}Cl\text{-}7\text{-}PtB_{10}H_{11}]$ in $CDCl_3$ solution at +20 °C: (*a*) spectrum with simultaneous {^{1}H} selective-decoupling irradiation at ν[^{1}H(bridge)]; (*b*) straightforward unperturbed spectrum; (*c*) difference between (*a*) and (*b*), showing that selective sharpening of the singlet resonance (plus its ^{195}Pt satellites) occurs in the ^{11}B-{^{1}H} experiment which therefore assigns this resonance and the site of SMe_2 substitution to B(8)

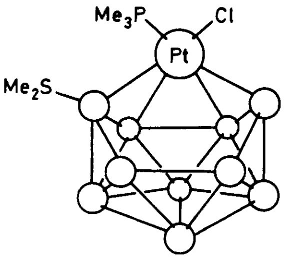

(4a)

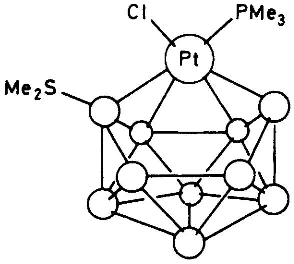

(4b)

therefore as depicted as (4) (*exo*-terminal H atoms omitted); on present evidence it is not possible to distinguish between *cisoid*, (4a), and *transoid*, (4b), mutual dispositions of the SMe_2 and PR_3 ligands, but the latter is probably favoured on steric grounds.

Additional points worth mentioning arising from the n.m.r. work are that the overall molecular asymmetry and slow inversion at the S atom result in chemical inequivalence of the two S–Me groups which thus give rise to separate ^{1}H n.m.r. signals for the SMe_2 compounds (Table 5); two resonance positions are similarly observed for the two P-methyl groups in the $Pt(PMe_2Ph)$ derivative. The molecule was difficult to assess for rotational fluxional behaviour (Figures 2 and 3), not least due to thermal instability; our observations were in

Table 7. Proton and boron-11 nuclear shieldings[a] in *arachno*-$(SMe_2)B_9H_{13}$ and *arachno*-$(SMe_2)_2B_{10}H_{12}$

	$4\text{-}(SMe_2)B_9H_{13}$			
Assignment[b]	$\delta(^{11}B)$ ($CDCl_3$)	$\delta(^{1}H)$ ($CDCl_3$)	$\delta(^{1}H)$ (C_6D_6)	$\Delta\sigma$(asis)[c]
(2), (3)	−39.2	+0.44	+1.27	−0.83
(4)	−23.3	+0.39[d]	+0.08[c]	+0.31[c]
(6), (8)	−21.5	+1.96[e]	+2.57[e]	−0.61
		−0.01[d,e]	+0.26[d,e]	−0.27[d]
(5), (9)	−16.3	+1.81	+2.13	−0.32
(1)	+4.4	+3.04	+3.38	−0.34
(7)	+18.1	+4.07	+4.64	−0.57
(5)/(9), (6)/(8)[f]	—	−3.53	−3.34	−0.19
SMe_2		+2.54	+1.36	+1.18

	$6,9\text{-}(SMe_2)_2B_{10}H_{12}$				
Assignment	$\delta(^{11}B)$ ($CDCl_3$)	$\delta(^{11}B)$ (C_6D_6)	$\delta(^{1}H)$ ($CDCl_3$)	$\delta(^{1}H)$ (C_6D_6)	$\Delta\sigma$(asis)[c]
(1), (3)	−40.1	−39.0	+0.40	+1.52	−1.12
(6), (9)	−23.0	−23.0	−0.37[d,g]	−0.13[d,g]	−0.24[d]
(5), (7), (8), (10)	−20.0	−19.0	+1.58	+2.24	−0.66
(2), (4)	−3.7	−2.7	+2.17	+2.81	−0.64
(5)/(10), (7)/(8)[f]	—	—	−4.71	−4.22	−0.49
SMe_2	—	—	+2.42	+1.59	+0.83

[a] $\delta(^{11}B)$ in p.p.m. (±0.5) to high frequency (low field) of $BF_3{\cdot}OEt_2$ (15% in $CDCl_3$); $\delta(^{1}H)$ in p.p.m. (±0.05) to high frequency (low field) of internal $SiMe_4$. [b] Assignments from ref. 33. [c] asis = aromatic solvent-induced shielding = $[\delta(^{1}H)(CDCl_3) - \delta(^{1}H)(C_6D_6)]$. Note δ and σ are of opposite sign. [d] *endo*-Terminal ^{1}H resonance. [e] Triplet structures, splittings *ca.* 10 Hz, presumably arising from couplings $^{n}J(^{1}H-^{1}H)$, $n = 2$ or 3 (*cf.* ref. 34*b*). [f] Bridging ^{1}H resonances. [g] Doublet, splitting *ca.* 5.8 Hz, presumably arising from a $^{3}J[^{1}H(6)(endo) - {}^{1}H(2)(exo)](transoid)$ coupling (*cf.* ref. 34*b*).

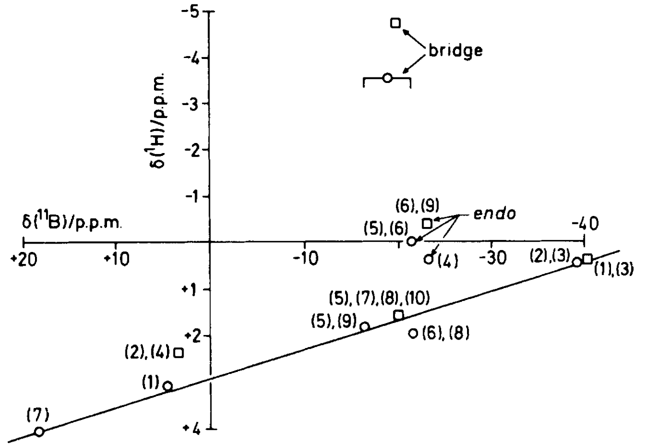

Figure 5. Plot of ^{1}H *versus* ^{11}B chemical shifts for directly bound atoms in $(SMe_2)B_9H_{13}$ (○) and $(SMe_2)_2B_{10}H_{12}$ (□); the line drawn has a gradient $\delta(^{1}H)/\delta(^{11}B)$ of 1/16. The proton chemical shifts are those measured in the non-aromatic solvent $CDCl_3$ (Table 7)

general consistent with either one PtB_4 rotamer or with a rapid equilibration of the two at all temperatures; we favour the former. Another point of interest is that the ^{31}P-{^{1}H(broad-band noise)} spectrum at higher temperatures exhibited considerable structure, presumably arising from the four vicinal couplings, $^{2}J(^{31}P-Pt-^{11}B)$; we have not attempted an analysis of this as the signal-to-noise ratio was poor under these conditions, but it was apparent that couplings of up to at least 40 Hz are involved. We have not previously observed this directly in any other phosphine-substituted platinaboranes that we have reported,[3-7,18-21,28] although a coupling of $^{2}J(^{31}P-Pt-^{11}B)$ of this magnitude has been estimated from consideration of the relaxation behaviour in $[Pt(B_5H_8)Cl(Ph_2PCH_2CH_2PPh_2)]$.[31] However, these other species were in general all larger molecules for which 'thermal decoupling' of the boron nuclei[31,32] will be more pronounced. Cooling of the $[7\text{-}Cl\text{-}7\text{-}(PR_3)\text{-}8\text{-}(SMe_2)\text{-}7\text{-}PtB_{10}H_{11}]$ species also resulted in 'thermal decoupling' of ^{11}B from the ^{31}P resonances;[27,32] for $PR_3 = PMe_2Ph$, in CD_2Cl_2 solution, $w_{\frac{1}{2}}$ at −40 °C was *ca.* 75 Hz with little fine structure apparent, and at −91 °C it was *ca.* 15 Hz with little deviation from essentially Lorentzian lineshape.

The *arachno* nine-vertex species $4\text{-}(SMe_2)B_9H_{13}$ and $4\text{-}(MeCN)B_9H_{13}$ produced in reactions (ii), (iiia), and (iiib), as mentioned above, were also identified by n.m.r. spectroscopy. The ^{11}B n.m.r. spectra of these compounds and related species have been very well characterized and assigned,[33] but their ^{1}H n.m.r. behaviour (in common with that of many otherwise well characterized polyhedral boron species) has not been previously reported.* As part of this work therefore we have also assigned the ^{1}H n.m.r. spectra of the *arachno* nine-vertex species $(SMe_2)B_9H_{13}$, and also the ten-vertex *arachno* species $(SMe_2)_2B_{10}H_{12}$, by selective ^{1}H-{^{11}B} n.m.r. spectroscopy,[3,19,26] and the results are summarized in Table 7. Although some more specific[7] and also more general[6] aspects of proton shielding correlations are dealt with elsewhere, that exhibited by the compounds in Table 7 is particularly illustrative of important general points which it is convenient to emphasize here. A plot of the proton *versus* the boron-11 shielding of the directly bonded atom is given in Figure 5, and the behaviour exhibited seems to be typical of many polyhedral boranes and metallaboranes: *exo*-terminal H atoms generally lie close to the line of slope 1/16 given in Figure 5[3,27] and the small deviations of up to *ca.* 1 p.p.m. that occur are of the magnitude expected from neighbour anisotropic and field effects, *etc.* For example, the somewhat higher shielding of H(2,4) in $(SMe_2)B_{10}H_{12}$ may well derive in this manner from the vicinal *cisoid* SMe_2 grouping [although if this is the case then it is difficult to see why H(1) in $(SMe_2)B_9H_{13}$ is not similarly shielded]. Larger deviations in general indicate an environment other than the straightforward *exo*-terminal. In the present case the *endo*-terminal H-atom resonances are *ca.* 2 p.p.m. above the *exo* plot, and the B–H–B bridging H atoms somewhat higher at *ca.* 5 p.p.m. above the *exo* plot. These are within typical ranges; M–H–B bridging proton resonances generally occur yet higher at >7—8 p.p.m. above the *exo* plot. With due allowance for any anisotropic substituent groups or solvents we often find this behaviour diagnostic; for example M–H–B bridging proton resonances are generally thought to resonate at particularly high fields (low frequencies) but, in fact, if they are bonded to a boron atom with a particularly low nuclear shielding (high frequency shift) then this need not necessarily be the case.

Additional interesting points arising out of this n.m.r. work are as follows. (*a*) The shielding patterns [except for the unique 7-position in $(SMe_2)B_9H_{13}$] for the two compounds are very similar, indicating that nine- and ten-vertex *arachno* species both have very similar cluster electronic structures.

(*b*) There are very marked solvent effects on proton shielding which occur on dissolution in benzene. These are characterized by an increase in shielding, $+\Delta\sigma$, of the S-methyl protons, and a decrease in shielding of all the borane *exo* protons. This indicates a strong association of the aromatic π-cloud with the SMe_2 methyl groups, and an association of the periphery of the aromatic ring with the cluster *exo*-terminal H atoms, and

---

* *Note added in proof*: see G. B. Jacobsen, J. H. Morris, and D. Reed, *J. Chem Soc., Dalton Trans.*, 1984, 415.

therefore suggests that the solute–solvent packing is substantially different from that proposed for *nido*-decaborane in aromatic solvents,[34a] in which the aromatic π-cloud is associated principally with the open face of the borane cluster.

(*c*) The proton spectra of $(SMe_2)B_9H_{13}$ and $(SMe_2)_2B_{10}H_{12}$ under conditions of complete ^{11}B decoupling exhibit fine structure arising from proton–proton coupling of which the most apparent are summarized in footnotes to Table 7. Similar couplings in *nido* ten-vertex systems have been examined in more detail and will be reported elsewhere.[34b]

Experimental

General.—The platinum(II) starting materials were prepared by standard literature methods [35,36] as were the borane adducts $(SMe_2)_2B_{10}H_{12}$, $(MeCN)_2B_{10}H_{12}$, $(PMe_2Ph)_2B_{10}H_{12}$,[37,38] and $(SMe_2)B_9H_{13}$.[39–41]

All the reactions were carried out under an inert atmosphere of dry deoxygenated nitrogen, but most of the subsequent manipulations were carried out in air. Preparative and analytical thin-layer chromatography (t.l.c.) were carried out using silica gel G (Fluka type GF 254) as the stationary phase, and the eluant was dichloromethane–light petroleum (b.p. 60—80 °C) (70 : 30), unless otherwise stated. All yields are based upon the platinum starting material, unless marked with an asterisk. I.r. spectra were recorded on a Perkin-Elmer 457 instrument and values quoted are ± 5 cm^{-1}.

Reaction of $[PtCl_2(PMe_2Ph)_2]$ *with* $(SMe_2)_2B_{10}H_{12}$.—(*a*) *In* CH_2Cl_2 *solution.* A solution of $[PtCl_2(PMe_2Ph)_2]$ (0.275 g, 0.51 mmol) and $(SMe_2)_2B_{10}H_{12}$ (0.134 g, 0.55 mmol) in CH_2Cl_2 (120 cm^3) was heated under reflux for 4 h or stirred for 36 h during which time the initially colourless solution turned yellow. The solvent and other volatile components were then removed under reduced pressure at 20—60 °C. The t.l.c. of a typical reaction mixture revealed eight components with major ones at $R_f = 0.74$, 0.58, 0.41, and 0.30. These compounds were separated by preparative-scale t.l.c. The component at $R_f = 0.74$ was shown to be $(SMe_2)B_9H_{13}$ by ^{11}B n.m.r. spectroscopy. The component at $R_f = 0.58$ was recrystallized as golden yellow plates from hot C_6H_{12}–CH_2Cl_2; an *X*-ray diffraction study showed them to be $[(PMe_2Ph)_2PtB_{10}H_{11}Cl]$ (see below).

Comparison of the ^{11}B n.m.r. spectrum of the component at $R_f = 0.41$ with those in the literature [3] showed it to be $[(PMe_2Ph)_2PtB_{10}H_{12}]$. Likewise that at $R_f = 0.30$ was shown to be the starting material, $(SMe_2)_2B_{10}H_{12}$. The minor components at $R_f = 0.92$, 0.90, 0.83, and 0.65 were not isolated. By comparison of analytical t.l.c. with those of authentic samples, *nido*-$B_{10}H_{14}$ was identified at $R_f = 0.90$ and that at $R_f = 0.65$ as *arachno*-$[(PMe_2Ph)_2PtB_8H_{12}]$. Isolated yields were for $[(PMe_2Ph)_2PtB_{10}H_{11}Cl]$, 57 mg (18%); $[(PMe_2Ph)_2PtB_{10}H_{12}]$, 17 mg (6%); $(SMe_2)B_9H_{13}$, 13 mg (13.5%) * {Found for $[(PMe_2Ph)_2PtB_8H_{11}Cl]$: C, 30.2; H, 5.3; B, 19.6; Cl, 5.1; P (by difference), 10.0; Pt, 29.9. Calc. for $C_{16}H_{33}B_{10}ClP_2Pt$: C, 30.7; H, 5.3; B, 17.3; Cl, 5.7; P, 9.9; Pt, 31.2%}; m.p. 170 °C (decomp.). I.r. (KBr disc) for $[(PMe_2Ph)_2PtB_{10}H_{11}Cl]$: 3 060 (w), 3 010 (w), 2 985 (w), 2 920 (m), 2 540 (s), 1 960 (w,br), 1 900 (w,br), 1 850 (w,br), 1 720 (m,br), 1 570 (w), 1 540 (m,br), 1 480 (m), 1 435 (s), 1 420 (m), 1 320 (m), 1 305 (m), 1 285 (m), 1 185 (w), 1 165 (w), 1 110 (m), 1 085 (m), 1 005 (s), 950 (s), 920 (s), 880 (w), 840 (m), 790 (w), 770 (w), 750 (s), 720 (s), 700 (s), 650 (w), 630 (m), 585 (w), 530 (m), 500 (s), 450 (w), 430 (m), and 370 (w) cm^{-1}.

(*b*) *In* CH_2Cl_2–Et_2O *solution.* The reaction of $[PtCl_2(PMe_2Ph)_2]$ (0.064 g, 0.12 mmol) and $(SMe_2)_2B_{10}H_{12}$ (0.03 g, 0.12 mmol) in CH_2Cl_2–Et_2O (1 : 1, 60 cm^3) was worked up as described above. Isolated yields were for $[(PMe_2Ph)_2PtB_{10}H_{11}Cl]$, 0.003 g (4%); $[(PMe_2Ph)_2PtB_8H_{12}]$, 0.010 g (15%); $[\{Pt(PMe_2Ph)(B_6H_9)\}_2]$ <1%; $B_{10}H_{14}$, trace identified by t.l.c.; $(SMe_2)B_9H_{13}$ (15%).*

Reaction of $[PtCl_2(PMe_2Ph)_2]$ *with* $(MeCN)_2B_{10}H_{12}$.—A solution of $[PtCl_2(PMe_2Ph)_2]$ (0.10 g, 0.18 mmol) and $(MeCN)_2B_{10}H_{12}$ (0.04 g, 0.20 mmol) in CH_2Cl_2 (40 cm^3) was heated under reflux for 5 h and then worked up as before. The products were identified by t.l.c. analysis and n.m.r. spectroscopy as $[(PMe_2Ph)_2PtB_{10}H_{11}Cl]$ (0.02 g, 15%), $[(PMe_2Ph)_2PtB_{10}H_{12}]$ (trace), and $(MeCN)B_9H_{13}$ (trace) ($R_f = 0.48$).

Reaction of $[PtCl_2(PMe_2Ph)_2]$ *with nido*-$B_{10}H_{14}$.—A solution of $[PtCl_2(PMe_2Ph)_2]$ (0.05 g, 0.09 mmol) and *nido*-$B_{10}H_{14}$ (0.01 g, 0.08 mmol) in CH_2Cl_2 (20 cm^3) was heated under reflux for 5 d. At the end of this time two components were observed by t.l.c. The component at $R_f = 0.41$, a yellow crystalline compound, was identified by n.m.r. spectroscopy as $[(PMe_2Ph)_2PtB_{10}H_{12}]$ (*ca.* 30 mg, *ca.* 60%) and that at $R_f = 0.90$ as unreacted $B_{10}H_{14}$.

Reactions of trans-$[\{PtCl_2(PR_3)\}_2]$ ($PR_3 = PMe_3$ *or* PMe_2Ph) *with* $(SMe_2)_2B_{10}H_{12}$.—A solution of $(SMe_2)_2B_{10}H_{12}$ (0.39 g, 1.60 mmol) and *trans*-$[\{PtCl_2(PMe_3)\}_2]$ (0.56 g, 0.82 mmol) in CH_2Cl_2 (50 cm^3) was stirred at *ca.* 20 °C for 36 h. The initially pale yellow solution turned orange. The volume of solvent was reduced to *ca.* 5 cm^3 on a Schlenk vacuum line. A t.l.c. of the mixture [eluant: CH_2Cl_2–light petroleum (b.p. 60—80 °C), 80 : 20] typically showed four spots at $R_f = 0.93$, 0.85, 0.56, and 0.43. These compounds were separated on a silica-gel column using the same eluant as above. The silica gel was baked in an oven for 3 d and all the solvents were dried, distilled and deoxygenated before use. Nitrogen was continuously bubbled into the top of the column in an attempt to prevent decomposition of the product.

The component at $R_f = 0.93$ was identified by comparative t.l.c. as *nido*-$B_{10}H_{14}$, that at 0.85 as $(SMe_2)B_9H_{13}$ and that at $R_f = 0.43$ as the starting material $(SMe_2)_2B_{10}H_{12}$. The component at $R_f = 0.56$ was collected off the column, the volume of solvent was reduced on a Schlenk line and then re-chromatographed using preparative t.l.c. with the same eluant and a nitrogen-enriched atmosphere. The yellow band was scraped off the t.l.c. plate, and the compound was extracted with CH_2Cl_2. Cyclohexane (10 cm^3) was added to the solution and the volume of solvent was reduced on the Schlenk line until the compound started to precipitate. The liquid was decanted, leaving behind the red decomposition product, and was then reduced to dryness giving a cream coloured solid, which was identified by n.m.r. spectroscopy and elemental analysis as $[(PMe_3)ClPtB_{10}H_{11}(SMe_2)]$. Isolated yields were for $[(PMe_3)ClPtB_{10}H_{11}(SMe_2)]$, 112 mg (14%); $B_{10}H_{14}$, 10 mg (5%);* $(SMe_2)B_9H_{13}$, 25 mg (9%) * (Found: C, 14.9; H, 6.05; B, 20.1; Cl, 8.9; P, 6.0; S, 6.2. Calc. for $C_5H_{26}B_{10}ClPPtS$: C, 12.3; H, 5.35; B, 22.2; Cl, 7.3; P, 6.4; S, 6.6%).

A solution of $[\{PtCl_2(PMe_2Ph)\}_2]$ (0.10 g, 0.12 mmol) and $(SMe_2)_2B_{10}H_{12}$ (0.06 g, 0.24 mmol) in CH_2Cl_2 (25 cm^3) was stirred for *ca.* 36 h and worked up as for the above reaction. The products were identified by n.m.r. spectroscopy as $B_{10}H_{14}$, $(SMe_2)B_9H_{13}$, $[(PMe_2Ph)ClPtB_{10}H_{11}(SMe_2)]$ (0.01 g, 15%, $R_f = 0.57$), and residual $(SMe_2)_2B_{10}H_{12}$.

Reaction of $[\{PtCl_2(PMe_2Ph)\}_2]$ *with* $(MeCN)_2B_{10}H_{12}$.—A solution of $(MeCN)_2B_{10}H_{12}$ (0.03 g, 0.15 mmol) and *trans*-$[\{PtCl_2(PMe_2Ph)\}_2]$ (0.10 g, 0.12 mmol) in CH_2Cl_2 (25 cm^3) was treated as in the analogous reactions of $(SMe_2)_2B_{10}H_{12}$. The products were identified as $B_{10}H_{14}$, $(MeCN)B_9H_{13}$, and $[(PMe_2Ph)ClPtB_{10}H_{11}(NCMe)]$ ($R_f = 0.33$). This latter compound was significantly less stable than its SMe_2 analogue and

Table 8. Fractional atomic co-ordinates, with estimated standard deviations in parentheses, for $[(PMe_2Ph)_2PtB_{10}H_{11}Cl]$

Atom	*X/a*	*Y/b*	*Z/c*	Atom	*X/a*	*Y/b*	*Z/c*
Pt(7)	0.663 03(5)	0.352 92(2)	0.592 12(4)	C(12)	0.413 0(7)	0.430 9(2)	0.666 5(7)
P(1)	0.523 0(2)	0.334 6(1)	0.713 7(2)	C(13)	0.357 3(7)	0.475 0(2)	0.696 4(7)
P(2)	0.853 8(2)	0.398 9(1)	0.769 3(2)	C(14)	0.355 7(7)	0.481 0(2)	0.824 0(7)
Cl	0.574 1(3)	0.226 1(1)	0.577 2(2)	C(15)	0.409 6(7)	0.442 9(2)	0.921 8(7)
B(1)	0.519 8(17)	0.339 0(4)	0.242 6(14)	C(16)	0.465 3(7)	0.398 8(2)	0.891 9(7)
B(2)	0.599 7(14)	0.381 7(4)	0.382 7(12)	Me(11)	0.332 6(12)	0.308 0(4)	0.616 8(11)
B(3)	0.486 8(14)	0.326 9(4)	0.387 5(12)	Me(12)	0.610 8(12)	0.294 7(4)	0.867 6(12)
B(4)	0.533 7(14)	0.275 9(4)	0.305 7(12)	Me(21)	0.861 6(13)	0.399 0(4)	0.945 4(12)
B(5)	0.671 8(16)	0.299 2(6)	0.253 4(13)	Me(22)	1.041 3(12)	0.374 9(4)	0.806 5(12)
B(6)	0.704 6(16)	0.363 5(6)	0.289 2(13)	C(21)	0.860 8(8)	0.465 7(2)	0.737 1(7)
B(8)	0.611 8(13)	0.277 7(4)	0.483 6(12)	C(22)	0.764 3(8)	0.497 7(2)	0.763 7(7)
B(9)	0.729 4(14)	0.261 2(4)	0.400 1(13)	C(23)	0.770 3(8)	0.549 2(2)	0.745 0(7)
B(10)	0.844 3(18)	0.319 3(6)	0.389 2(14)	C(24)	0.873 0(8)	0.568 6(2)	0.699 6(7)
B(11)	0.803 6(14)	0.374 5(4)	0.471 5(12)	C(25)	0.969 5(8)	0.536 5(2)	0.673 0(7)
C(11)	0.466 9(7)	0.392 8(2)	0.764 2(7)	C(26)	0.963 5(8)	0.485 1(2)	0.691 7(7)

was not isolated in a significant quantity. Estimated yield, *ca.* 70%.

X-Ray Diffraction Analysis.—Recrystallization of [8-Cl-7,7-$(PMe_2Ph)_2$-*nido*-7-$PtB_{10}H_{11}$] from hot dichloromethane–cyclohexane yielded golden yellow plates suitable for single-crystal *X*-ray diffraction analysis.

Crystal data. $C_{16}H_{33}B_{10}ClP_2Pt$, $M = 626.03$, monoclinic, $a = 978.9(2)$, $b = 2\,674.3(7)$, $c = 1\,079.6(2)$ pm, $\beta = 115.83(2)°$, $U = 2.544(1)$ nm^3, $Z = 4$, $D_c = 1.634$ g cm^{-3}, $F(000) = 1\,216$, space group $P2_1/n$, Mo-K_α radiation, $\lambda = 71.069$ pm, μ(Mo-K_α) = 5.806 mm^{-1}.

Structure determination. Measurements were made on a Syntex $P2_1$ diffractometer. Cell dimensions were determined by least-squares treatment of the setting angles of 15 reflections with $35 < 2\theta < 40°$. Intensities of all independent reflections with $4 < 2\theta < 45°$ were measured in the ω–2θ scan mode with scan speeds varying between 3.9 and 29.3° min^{-1} according to a pre-scan intensity and running from 1° below $K_{\alpha1}$ to 1° above $K_{\alpha2}$. The structure analysis used the 2 628 reflections having $I > 2\sigma(I)$; 725 below this threshold were rejected as 'unobserved'. Correction for Lorentz, polarization, and transmission factors, solution using Patterson and difference syntheses, and full-matrix least-squares refinement with anisotropic temperature factors for Pt, P, and Cl and isotropic parameters for C and B gave $R = 0.041$.

Atomic scattering factors were calculated using the analytical approximation and coefficients tabulated in ref. 42. Final atomic co-ordinates and estimated standard deviations are listed in Table 8. The molecular structure and atom numbering are shown in Figure 1.

N.M.R. Experiments.—Proton (100 MHz), ^{31}P (40 MHz), and ^{11}B (32 MHz) n.m.r. work was carried out on a JEOL FX-100 instrument in these laboratories, and ^{11}B work at 128 MHz on the S.E.R.C. Bruker WH 400 service instrument at the University of Sheffield. Chemical shifts $\delta(^{31}P)$ and $\delta(^{11}B)$ are quoted in p.p.m. to high frequency (low field) of 85% H_3PO_4 (Ξ = 40 480 730 Hz) and $BF_3\cdot Et_2O$ (15% v/v in $CDCl_3$) (Ξ = 32 083 971 Hz). The technique of selective multiple resonance as applied to this work is adequately described elsewhere.[3,19,27,34b]

Acknowledgements

We thank the S.E.R.C. for support and Dr. B. E. Mann (Sheffield University) for services in high-field n.m.r. spectroscopy.

References

1 N. N. Greenwood and J. D. Kennedy, 'Metal Interactions with Boron Clusters,' ed. R. N. Grimes, Plenum Press, New York, 1982, ch. 2, pp. 43—118.

2 S. K. Boocock, N. N. Greenwood, and J. D. Kennedy, *J. Chem. Soc., Chem. Commun.*, 1980, 305.

3 J. D. Kennedy and B. Wrackmeyer, *J. Magn. Reson.*, 1980, **38**, 529.

4 S. K. Boocock, N. N. Greenwood, J. D. Kennedy, W. S. McDonald, and J. Staves, *J. Chem. Soc., Dalton Trans.*, 1981, 2573.

5 Y. M. Cheek, N. N. Greenwood, J. D. Kennedy, and W. S. McDonald, *J. Chem. Soc., Chem. Commun.*, 1982, 80.

6 N. N. Greenwood, M. J. Hails, J. D. Kennedy, and W. S. McDonald, *J. Chem. Soc., Dalton Trans.*, in the press.

7 R. Ahmad, N. N. Greenwood, and J. D. Kennedy, unpublished work; see also R. Ahmad, Ph.D. Thesis, University of Leeds, 1982.

8 R. Schaeffer, *J. Am. Chem. Soc.*, 1957, **79**, 1006.

9 T. E. Paxson and M. F. Hawthorne, *Inorg. Chem.*, 1975, **14**, 1604.

10 A. R. Siedle and T. A. Hill, *J. Inorg. Nucl. Chem.*, 1969, **31**, 3874.

11 R. M. Adams, *Pure Appl. Chem.*, 1972, **30**, 683.

12 W. H. Knoth and E. L. Muetterties, *J. Inorg. Nucl. Chem.*, 1961, **20**, 66.

13 B. Štíbr, J. Plešek, and S. Heřmánek, *Collect. Czech. Chem. Commun.*, 1972, **37**, 2696.

14 W. E. Hill, F. A. Johnson, and R. W. Novak, *Inorg. Chem.*, 1975, **14**, 1244.

15 E. I. Tolpin, E. Mizusawa, D. S. Becker, and J. Venzel, *Inorg. Chem.*, 1980, **19**, 1182.

16 S. K. Boocock, N. N. Greenwood, J. D. Kennedy, W. S. McDonald, and J. Staves, *J. Chem. Soc., Dalton Trans.*, 1980, 790.

17 W. E. Hill, F. A. Johnson, and N. S. Hosmane, 'Boron Chemistry-4,' eds. R. W. Parry and G. Kodama, Pergamon, 1980, pp. 33—39.

18 N. N. Greenwood, M. J. Hails, J. D. Kennedy, and W. S. McDonald, *J. Chem. Soc., Chem. Commun.*, 1980, 37.

19 S. K. Boocock, N. N. Greenwood, M. J. Hails, J. D. Kennedy, and W. S. McDonald, *J. Chem. Soc., Dalton Trans.*, 1981, 1415.

20 R. Ahmad, PhD. Thesis, University of Leeds, 1982.

21 R. Ahmad, J. E. Crook, N. N. Greenwood, J. D. Kennedy, and W. S. McDonald, *J. Chem. Soc., Chem. Commun.*, 1982, 1019.

22 B. Štíbr, J. Plešek, and S. Heřmánek, *Collect. Czech. Chem. Commun.*, 1969, **34**, 194.

23 J. Plešek, B. Štíbr, and S. Heřmánek, *Collect. Czech. Chem. Commun.*, 1966, **31**, 4744.

24 P. Sedmera, F. Hanousek, and Z. Samek, *Collect. Czech. Chem. Commun.*, 1968, 33, 2169.

25 J. Plešek, S. Heřmánek, and B. Štíbr, *Collect. Czech. Chem. Commun.*, 1972, **37**, 2696.

26 M. A. Beckett and J. D. Kennedy, *J. Chem. Soc., Chem. Commun.*, 1983, 575.

27 J. D. Kennedy and N. N. Greenwood, *Inorg. Chim. Acta*, 1980, **38**, 93.

28 N. N. Greenwood, J. D. Kennedy, and J. Staves, *J. Chem. Soc., Dalton Trans.*, 1978, 1146.

29 J. D. Kennedy, I. J. Colquhoun, W. McFarlane, and R. J. Puddephatt, *J. Organomet. Chem.*, 1979, **172**, 479 and refs. therein.

30 D. A. Thompson, T. K. Hilty, and R. W. Rudolph, *J. Am. Chem. Soc.*, 1977, **99**, 6774.

31 J. D. Kennedy and J. Staves, *Z. Naturforsch., Teil B*, 1979, **34**, 808.

32 M. Grace, H. Beall, and C. H. Bushweller, *Chem. Commun.*, 1970, 701.

33 L. J. Todd, G. M. Bodner, F. R. Scholer, L. E. Senor, and J. C. Carter, *Inorg. Chem.*, 1971, **10**, 942.

34 (*a*) T. C. Gibb and J. D. Kennedy, *J. Chem. Soc., Faraday Trans. 2*, 1982, 525; (*b*) M. A. Beckett and J. D. Kennedy, unpublished work.

35 G. B. Kauffman and D. O. Cowan, *Inorg. Synth.*, 1960, **6**, 211; G. B. Kauffman and L. A. Teter, *ibid.*, 1963, **7**, 245; G. W. Parshall, *ibid.*, 1970, **12**, 27; A. C. Smithies, P. Schmidt, and M. Orchin, *ibid.*, p. 240.

36 K. A. Jensen, *Z. Anorg. Allg. Chem.*, 1936, **229**, 242.

37 R. Schaeffer, *J. Am. Chem. Soc.*, 1957, **79**, 1006.

38 R. J. Pace, J. Williams, and R. L. Williams, *J. Chem. Soc.*, 1961, 2198.

39 B. M. Graybill, A. R. Pitochelli, and M. F. Hawthorne, *Inorg. Chem.*, 1962, **1**, 626.

40 B. M. Graybill, J. K. Ruff, and M. F. Hawthorne, *J. Am. Chem. Soc.*, 1961, **83**, 2669.

41 S. Heřmánek, J. Plešek, B. Štíbr, and F. Hanousek, *Collect. Czech. Chem. Commun.*, 1968, **33**, 2177.

42 'International Tables for *X*-Ray Crystallography,' Kynoch Press, Birmingham, 1974, vol. 4.

Received 8*th February* 1984; *Paper* 4/227